ISSN : 2350-0743

International Journal of Recent Advances in Multidisciplinary Research

Vol. 12, Issue 09, pp.11737-11746, September, 2025

https://doi.org/10.64485/ijramr.6080.09.2025

RESEARCH ARTICLE **CROSSREF** **OPEN ACCESS**

ESTIMATION OF CAPACITY BETWEEN THE TRUNCATED CONE AND THE METAL PLATE BY METHOD OF MOMENTS

Chol-Min An, Sung-Pok Jo, Gwang-Hyok Kim and *Yong-Jun Kim

Faculty of Physical Engineering, Kim Chaek University of Technology, Democratic People's Republic of Korea

ARTICLE INFO

Article History

Received 24th June, 2025
Received in revised form
28th July, 2025
Accepted 24th August, 2025
Published online 30th September, 2025

Keywords:

Truncated Cone; Method of Moments; Point Matching; Capacity Estimation.

Corresponding author:
Yong-Jun Kim

ABSTRACT

We present a method for the evaluation of the capacitance and charge distribution between the metallic truncated cone of finite length with bottom and the grounded metallic plate. The estimation of capacitance and charge distribution is carried out using the method of moments (MoM) based on pulse function as the basis function and point matching for testing. The matrix elements to be inverted in the solving process are found by dividing the surfaces of the truncated cone and the metallic plate into subsections. The capacitance and the charge distribution are derived from the inverse matrix. Numerical results on the capacitance and charge distribution between the metallic truncated cone of finite length with bottom and the grounded metallic plate are compared with the experimental data.

Citation: Chol-Min An, Sung-Pok Jo, Gwang-Hyok Kim and Yong-Jun Kim, 2025. "Estimation of capacity between the truncated cone and the metal plate by Method of Moments", International Journal of Recent Advances in Multidisciplinary Research, 11, (09), 11737-11746.

INTRODUCTION

Electrostatic models for the evaluation of the capacitance and charge distribution of various geometrical shaped metallic objects have been widely studied. Harrington (1993) analyzed the capacitance of a cylinder with finite height, dividing the cylinder into sub-cylindrical sections, and dividing the sections into square sections again, and then employing the moment method. However, he did propose an explicit expression for the capacitance and charge distribution of the cylinder. This technique is further complicated to apply to the truncated cone. Work by Savage and Smith(1995) showed that when analyzing the above structures, the assumption of axial charge distribution instead of surface charge distribution of the metallic structures was made, which is valid only for cylinders of infinite length and does not converge for cylinders or truncated cones of finite length. In some works (Das et al. 1995;Mehta et al. 2013; Das et al. 1997), analyzing the capacitance and charge distribution of the cylinder and truncated cone structure, the structure was first divided into sub-cylinders with the same axial length, again these subsections were divided into curvilinear rectangular subsections and then the numerical results were obtained by the method of moments. These resultswere considered for the case of a relatively large height-to-radius ration, and no study of a small height-to-radius ration has been considered in recent works (Pal et al. 2020; Ubezio et al. 2023; Hanni et al. 2020; Abdelhamid et al. 2022; Fu et al. 2020). In this paper, we deal with the truncated cone with a low height-to-radius. We divide the side and bottom surfaces of the truncated cone into sub annular sections and again divide the sub annular sections into curvilinear rectangles and analyze them. The total system consists of a truncated cone with anannularbottom and a grounded metal plate at a distance from it. The unknown charge distribution of the side and bottom surfaces of the truncated cone is expressed in the form of an integral equation relating the potential function and the charge distribution. The expressions determining the matrix elements are established. The method of moments based on the pulse basis function and point matching is used to calculate the capacitance and charge distribution in the truncated cone surface. The calculated numerical results are compared with the experimental values.

Analysis: Fig. 1 shows the geometry of the metal plate and the structure of the truncated cone considered where $R_0$and $R_1$are the inner and outer radii of the bottom surface of the truncated cone, $R_2$is the upper radius of the truncated cone, R_3 is the radius of the metal plate, $d$is the distance betweenthe bottom surface of the truncated cone and the metal plate, and $h$is the height of the

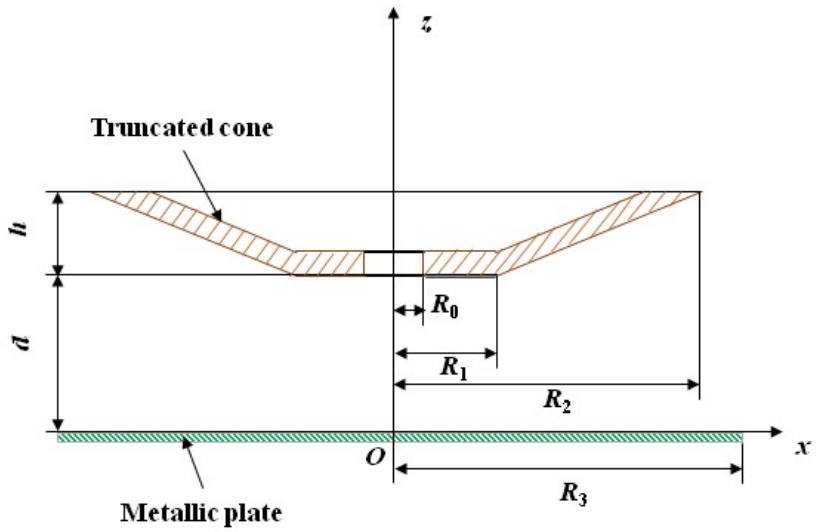

Fig. 1. Structure of the truncated cone and the metallic plate

truncated cone. According to the electrostatic theory, the potential at any point in space is expressed by the superposition of the potentials that all the elementary charges make at that point (Hwang et al. 2004), and so we have

$$V = \int_{S_1} \frac{\sigma_1(\vec{r}')}{4\pi\varepsilon|\vec{r}-\vec{r}'|} ds' + \int_{S_2} \frac{\sigma_2(\vec{r}')}{4\pi\varepsilon|\vec{r}-\vec{r}'|} ds' + \int_{S_3} \frac{\sigma_3(\vec{r}')}{4\pi\varepsilon|\vec{r}-\vec{r}'|} ds' \quad (1)$$

where $\vec{r}$ and $\vec{r}'$ are the position vectors corresponding to observation and charge source points respectively, ds' is an element area on the side surface $S_1$of truncated cone, the bottom surfaceS_2 of the truncated cone, and the metal plate surfaceS_3.ε is the permittivity between the truncated cone and the metal plate, $\sigma_1(\vec{r}')$, $\sigma_2(\vec{r}')$, $\sigma_3(\vec{r}')$ are the charge densities on S_1, $S_2$and S_3. In general, it is difficult to find the solution of this equation, so that the three surfaces can be divided into elementary surfaces and solved numerically. In the works (Das et al. 1995; Mehta et al. 2013; Das et al. 1997), the truncated cone was subdivided into sub-cylinders, where the height $h$of the truncated cone is significantly larger than the radii R_1, $R_2$of the top and bottom surfaces. In this paper, R_2 is much larger than R_1 and h, so we divide the side surface of the truncated cone into sub annular sections instead of sub cylindrical sections. The bottom surface of the truncated cone and the metal plate are also divided into sub annular sections.

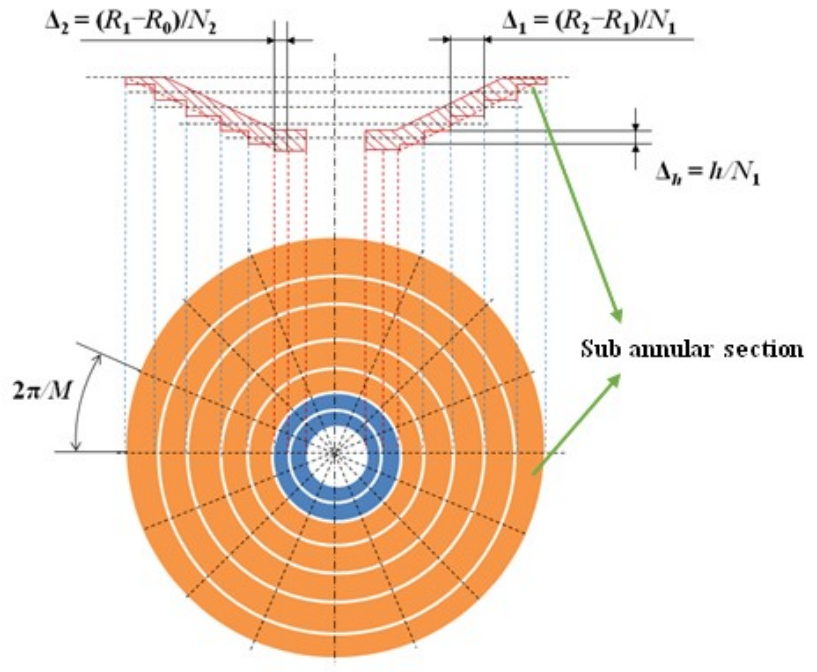

Fig. 2. Sub annular sections of the truncated cone

In Fig. 2, the method of dividing the side and the bottom surfaces of the truncated cone is shown. Let N_1represent the number of radial divisions of S_1, $N_2$the number of radial divisions of S_2, and$N_3$the number of radial divisions of S_3, and the radial interval in each section is Δ_1= (R_2-R_1)/N_1, Δ_2= (R_1-R_0)/N_2andΔ_3 = R_3/N_3. The height interval of the sub annular sections on the side surface of

the truncated cone is $\Delta_h = h/N_1$. The sub annular sections are further divided by the planes passing through the z-axis along the circumferential direction. The angle between these planes is $2\pi/M$. The surface $S_1$is divided into $M\times N_1$elements, S_2surface into $M\times N_2$elements and S_3surface into $M\times N_3$elements. The number of elements in S_1, $S_2$and $S_3$is plotted counterclockwise starting from the innermost sub annular section as shown in Fig. 3.

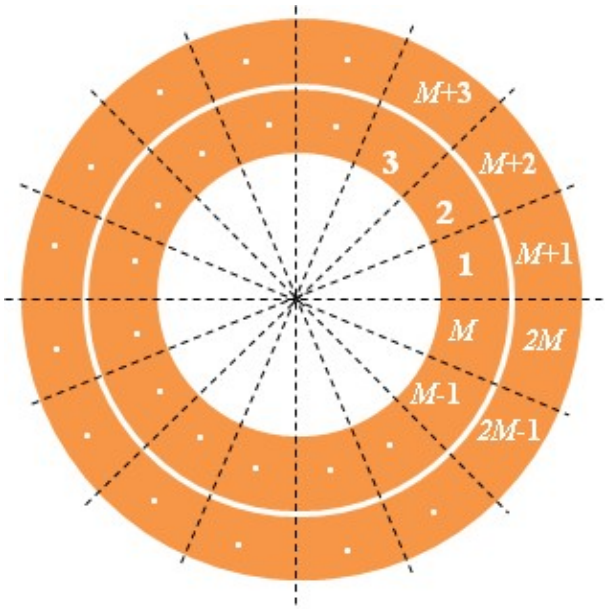

Fig. 3. Element numbering

-If the considered element is on the side surface S_1,

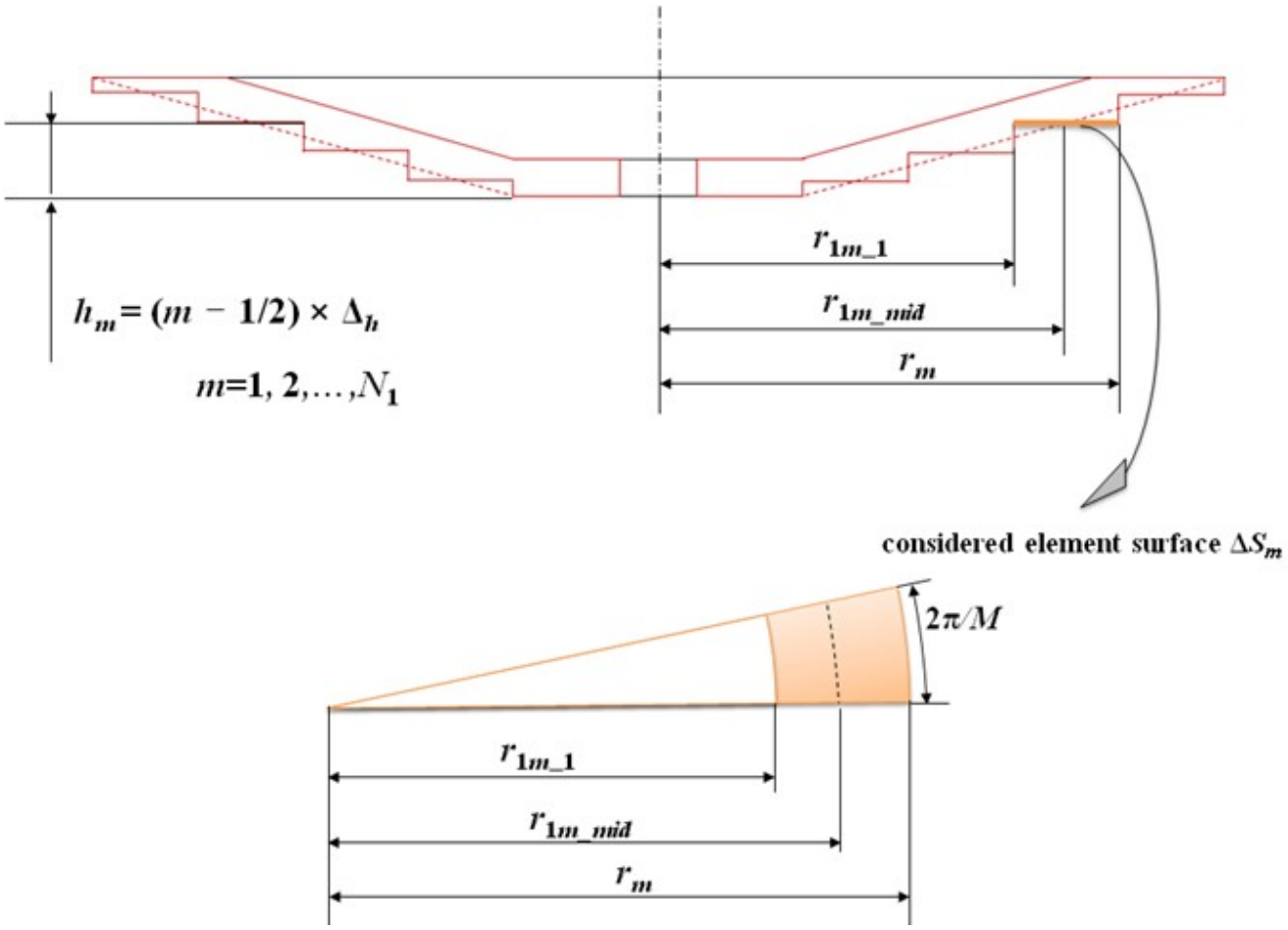

Fig. 4. Shape of the element surface on the side of the truncated cone

In the figure,

$$\begin{cases} r_{1m} = R_1 + m \times \Delta_1 \\ r_{1m\_mid} = R_1 + \left(m - \dfrac{1}{2} \right) \times \Delta_1 \\ r_{1m\_1} = R_1 + (m-1) \times \Delta_1 \\ h_m = \left(m - \dfrac{1}{2} \right) \times \Delta_h \end{cases} \tag{2}$$

m=1, 2,...,N_1

-If the considered element is on the surface S_2,

$$\begin{cases} r_{2m} = R_0 + m \times \Delta_2 \\ r_{2m\_mid} = R_0 + \left(m - \dfrac{1}{2} \right) \times \Delta_2 \\ r_{2m\_1} = R_0 + (m-1) \times \Delta_2 \end{cases} \tag{3}$$

m=1, 2,...,N_2

-If the considered element is on the surface S_3,

-

$$\begin{cases} r_{3m} = m \times \Delta_3 \\ r_{3m\_mid} = \left(m - \dfrac{1}{2} \right) \times \Delta_3 \\ r_{3m\_1} = (m-1) \times \Delta_3 \end{cases} \tag{4}$$

m=1, 2,...,N_3

To determine the location of the element, the position angle as well as radius must be given. Let the angle between the radial vector of the center point of the element and the x-axis represent the position angle θ_m.

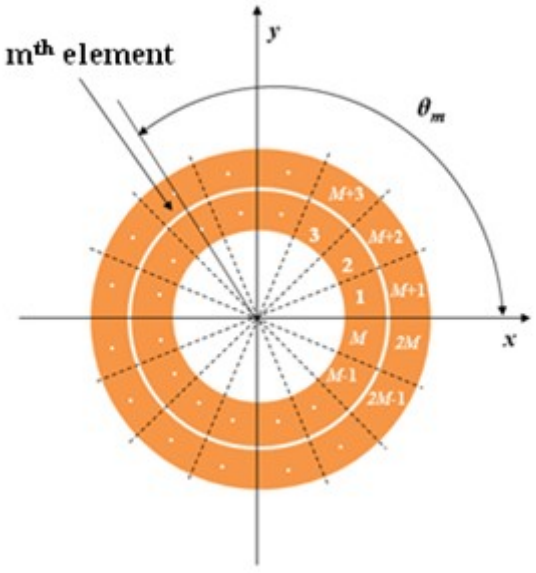

Fig. 5. Position angle of element surface

According to the numbering method of elements, the position angle and radius of the m^{th} element of the i^{th} surfacehave the relationship of$\theta_m = \theta_\xi$ and$r_m = r_l$when $m=kM+\xi$, $m=lM-\eta$ and $h_m = h_l$on the surfaceS_1.

Here

i=1, 2, 3
m=1, 2, ..., MN_i
k=0, 1, … , N_i-1
ξ=1, 2, … , M
l=1, 2, … , N_i
η =0, 1, … , M-1

Based on the above dividing, we will calculate the charge distribution and capacitance between the truncated cone and the metal plate by MoM using pulse basis function and point matching. The potentials on the side and bottom surfaces of the truncated cone are given as V_1= V_2=V and the potential $V_3$of the metal plate is 0. Eq. (1) can be expressed for any observation point located in S_1, S_2 and S_3 as follows:

$$V_i(\vec{r}_i)=\sum_{j=1}^{3}\int_{s_j}\frac{1}{4\pi\varepsilon_0}\frac{\sigma_j(\vec{r}_j')ds}{\left|\vec{r}_i-\vec{r}_j'\right|} \tag{5}$$

$\vec{r}_i$, $\vec{r}_j'$: Position vectors corresponding to observation and charge source points.

$V_i(\vec{r}_i)$: Potential of the observation point on surface S_i

$\sigma_j(\vec{r}_j')$: Charge density at the charge source point on surfaceS_j

Then, $\sigma_j$can be expressed in terms of pulse basis functionsas

$$\sigma_j(\vec{r}_j)=\sum_{n=1}^{MN_j}\sigma_{jn}f_n\ ;\qquad j=1,2,3 \tag{6}$$

where$\sigma_{jn}$is charge density on them^{th} element of the i^{th} surface. $f_n$are the pulse functions given by

$$f_n=\begin{cases}1, & \in \Delta s_n\\ 0, & \notin \Delta s_n\end{cases}$$

The potential at the center of any element surface has the following form(Chakrabarty et al. 2002)

$$V_{im}=\sum_{j=1}^{3}\sum_{n=1}^{MN_i}\sigma_{jn}l_{ijmn} \tag{7}$$

V_{1m}, V_{2m}, V_{3m}:Potential at the center of the m^{th} element surface in S_1, S_2 and S_3

l_{ijmn}: Potential at the center of m^{th} element of the i^{th} surface due to a uniform charge density of unit amplitude over n^{th} element of the j^{th}surface.(i,j=1,2,3)

$$V=\sum_{n=1}^{MN_1}\sigma_{1n}l_{11mn}+\sum_{n=1}^{MN_2}\sigma_{2n}l_{12mn}+\sum_{n=1}^{MN_3}\sigma_{3n}l_{13mn} \tag{8}$$

$$V=\sum_{n=1}^{MN_1}\sigma_{1n}l_{21mn}+\sum_{n=1}^{MN_2}\sigma_{2n}l_{22mn}+\sum_{n=1}^{MN_3}\sigma_{3n}l_{23mn} \tag{9}$$

$$0=\sum_{n=1}^{MN_1}\sigma_{1n}l_{31mn}+\sum_{n=1}^{MN_2}\sigma_{2n}l_{32mn}+\sum_{n=1}^{MN_3}\sigma_{3n}l_{33mn} \tag{10}$$

Now, we need to findl_{ijmn}in detail. Let ΔS_{1n}, ΔS_{2n} andΔS_{3n}represent the element areas of the n^{th} element in S_1, $S_2$and S_3.

$$\Delta s_{in}=\frac{\pi}{M}\left(r_{in}^2-r_{in\_1}^2\right)i\text{=}1,2,3 \tag{11}$$

The definition ofr_{in} in surfaces S_1, S_2 and S_3 refer to Eqs.(2)-(4), respectively.

For surfaces S_1, S_2 andS_3, if m=n, i.e., the center of the source element is the observation point, the element can be approximated as a rectangle as shown in Fig. 6. Then we have

$$l_{iinn}=\frac{1}{4\pi\varepsilon_0}\int_{-\pi r_{in\_mid}/M}^{\pi r_{in\_mid}/M}\int_{-\Delta_i/2}^{\Delta_i/2}\frac{dxdy}{\sqrt{x^2+y^2}}=$$

$$\frac{1}{2\pi\varepsilon_0}\left(\frac{\Delta_i}{2}\ln\frac{\sqrt{\left(\frac{\Delta_i}{2}\right)^2+\left(\frac{\pi r_{in\_mid}}{M}\right)^2}+\frac{\pi r_{in\_mid}}{M}}{\sqrt{\left(\frac{\Delta_i}{2}\right)^2+\left(\frac{\pi r_{in\_mid}}{M}\right)^2}-\frac{\pi r_{in\_mid}}{M}}+\frac{\pi r_{in\_mid}}{M}\ln\frac{\sqrt{\left(\frac{\Delta_i}{2}\right)^2+\left(\frac{\pi r_{in\_mid}}{M}\right)^2}+\frac{\Delta_i}{2}}{\sqrt{\left(\frac{\Delta_i}{2}\right)^2+\left(\frac{\pi r_{in\_mid}}{M}\right)^2}-\frac{\Delta_i}{2}}\right)\quad i=1,2,3 \tag{12}$$

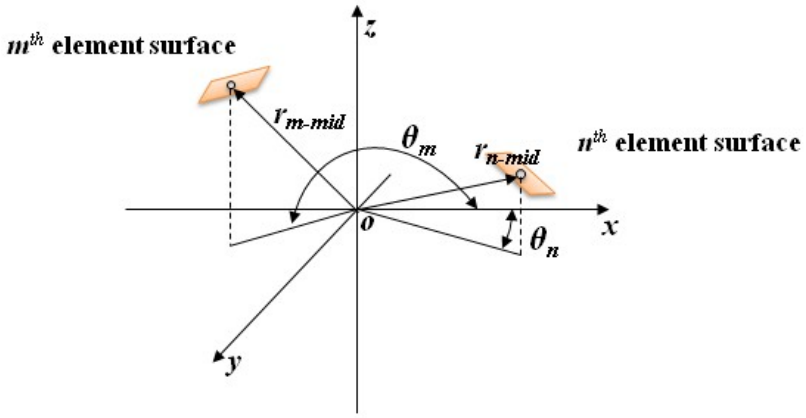

Fig.7. Considered m^{th} and n^{th} element surface

In the case of $m\neq n$, the angle between the m^{th} and n^{th} element surfaces is

$$\theta=\theta_m-\theta_n=\frac{2\pi}{M}(m-n) \tag{13}$$

And the potential at the center of m^{th} element produced by unit charge density of n^{th}element on the surface $S_1$is

$$l_{11mn}=\frac{1}{4\pi\varepsilon_0}\frac{\Delta s_{1n}}{|\vec{r}_{1m}-\vec{r}_{1n}|}=\frac{1}{4\pi\varepsilon_0}\frac{\Delta s_{1n}}{\sqrt{r_{1m\_mid}^2+r_{1n\_mid}^2-2r_{1m\_mid}r_{1n\_mid}\cos\theta+(h_m-h_n)^2}} \tag{14}$$

If $m\neq n$ on the surfaceS_2,

$$l_{22mn}=\frac{1}{4\pi\varepsilon_0}\frac{\Delta s_{2n}}{|\vec{r}_{2m}-\vec{r}_{2n}|}=\frac{1}{4\pi\varepsilon_0}\frac{\Delta s_{2n}}{\sqrt{r_{2m\_mid}^2+r_{2n\_mid}^2-2r_{2m\_mid}r_{2n\_mid}\cos\theta}} \tag{15}$$

And if $m\neq n$ on the surface S_3,

$$l_{33mn}=\frac{1}{4\pi\varepsilon_0}\frac{\Delta s_{3n}}{|\vec{r}_{3m}-\vec{r}_{3n}|}=\frac{1}{4\pi\varepsilon_0}\frac{\Delta s_{3n}}{\sqrt{r_{3m\_mid}^2+r_{3n\_mid}^2-2r_{3m\_mid}r_{3n\_mid}\cos\theta}} \tag{16}$$

Likewise, we can find that

$$l_{12mn}=\frac{1}{4\pi\varepsilon_0}\frac{\Delta s_{2n}}{|\vec{r}_{1m}-\vec{r}_{2n}|}=\frac{1}{4\pi\varepsilon_0}\frac{\Delta s_{2n}}{\sqrt{r_{1m\_mid}^2+r_{2n\_mid}^2-2r_{1m\_mid}r_{2n\_mid}\cos\theta+h_m^2}} \tag{17}$$

$$l_{13mn}=\frac{1}{4\pi\varepsilon_0}\frac{\Delta s_{3n}}{|\vec{r}_{1m}-\vec{r}_{3n}|}=\frac{1}{4\pi\varepsilon_0}\frac{\Delta s_{3n}}{\sqrt{r_{1m\_mid}^2+r_{3n\_mid}^2-2r_{1m\_mid}r_{3n\_mid}\cos\theta+(h_m+d)^2}} \tag{18}$$

$$l_{21mn}=\frac{1}{4\pi\varepsilon_0}\frac{\Delta s_{1n}}{|\vec{r}_{2m}-\vec{r}_{1n}|}=\frac{1}{4\pi\varepsilon_0}\frac{\Delta s_{1n}}{\sqrt{r_{2m\_mid}^2+r_{1n\_mid}^2-2r_{2m\_mid}r_{1n\_mid}\cos\theta+h_n^2}} \tag{19}$$

$$l_{23mn}=\frac{1}{4\pi\varepsilon_0}\frac{\Delta s_{3n}}{|\vec{r}_{2m}-\vec{r}_{3n}|}=\frac{1}{4\pi\varepsilon_0}\frac{\Delta s_{3n}}{\sqrt{r_{2m\_mid}^2+r_{3n\_mid}^2-2r_{2m\_mid}r_{3n\_mid}\cos\theta+d^2}} \tag{20}$$

$$l_{31mn}=\frac{1}{4\pi\varepsilon_0}\frac{\Delta s_{1n}}{|\vec{r}_{3m}-\vec{r}_{1n}|}=\frac{1}{4\pi\varepsilon_0}\frac{\Delta s_{1n}}{\sqrt{r_{3m\_mid}^2+r_{1n\_mid}^2-2r_{3m\_mid}r_{1n\_mid}\cos\theta+(h_n+d)^2}} \tag{21}$$

$$l_{32mn}=\frac{1}{4\pi\varepsilon_0}\frac{\Delta s_{2n}}{|\vec{r}_{3m}-\vec{r}_{2n}|}=\frac{1}{4\pi\varepsilon_0}\frac{\Delta s_{2n}}{\sqrt{r_{3m\_mid}^2+r_{2n\_mid}^2-2r_{3m\_mid}r_{2n\_mid}\cos\theta+d^2}} \tag{22}$$

Expressing Eqs.(8)-(10)in matrix form,

$$\begin{bmatrix}[l_{11mn}][l_{12mn}][l_{13mn}]\\[l_{21mn}][l_{22mn}][l_{23mn}]\\[l_{31mn}][l_{32mn}][l_{33mn}]\end{bmatrix}\begin{bmatrix}[\sigma_{1n}]\\[\sigma_{2n}]\\[\sigma_{2n}]\end{bmatrix}=\begin{bmatrix}[V]\\[V]\\[0]\end{bmatrix} \tag{23}$$

Substituting Eqs.(14)–(22) into Eq. (23) and multiplying the right-hand side of Eq. (23) by the inverse matrix of $[l_{ijmn}]$ yields $[\sigma_{in}]$. Then, the charge and capacitance can be found as follows:

$$C=\frac{Q}{V}=\left(\sum_{n=1}^{MN_1}\sigma_{1n}\Delta s_{1n}+\sum_{n=1}^{MN_2}\sigma_{2n}\Delta s_{2n}\right)\cdot\frac{1}{V} \tag{24}$$

The charge distributions calculated using MATLAB 16.0a for d=0.1mm, 0.5mm, 1mm and 2mm are shown in Fig. 8 where V=5V, R_0=3mm, R_1=8mm, R_2=20mm, h=10mm, R_3=2m, M=120, N_1=16, N_2=16, N_3=40.

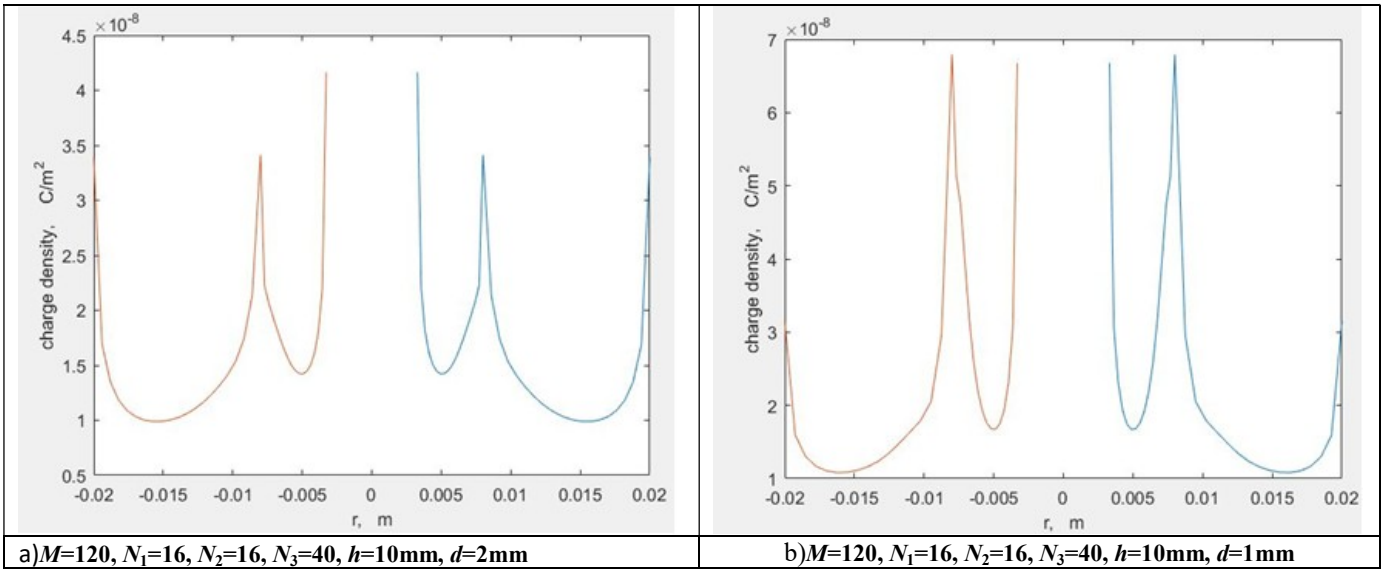

a)**M=120, N_1=16, N_2=16, N_3=40, h=10mm, d=2mm** | b)**M=120, N_1=16, N_2=16, N_3=40, h=10mm, d=1mm**

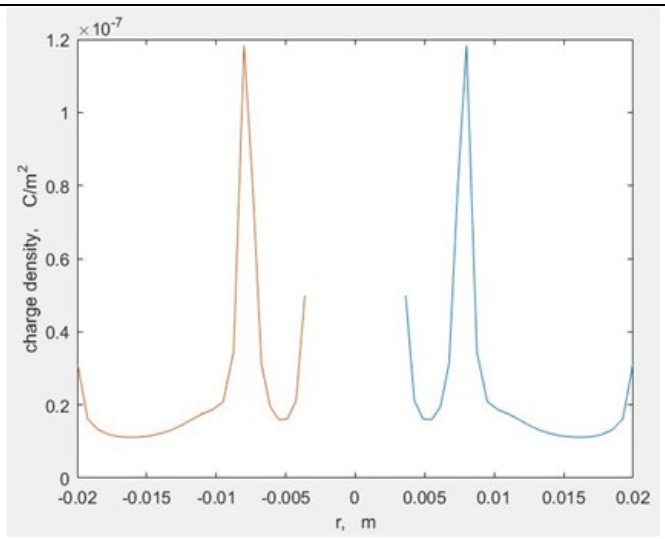

c)M=120, N_1=16, N_2=16, N_3=40, h=10mm, d=0.5mm

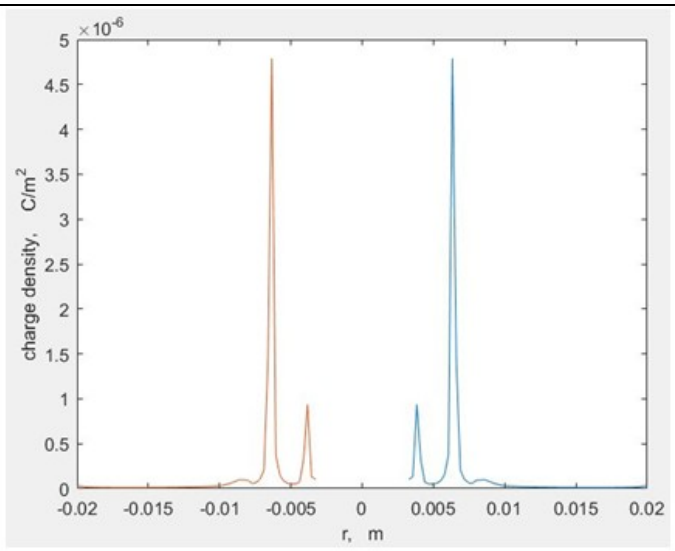

d) M=120, N_1=16, N_2=16, N_3=40, h=10mm, d=0.1mm

Fig.8. Radial charge distribution in the truncated cone

As can be seen from the figure, the calculatedresults show well the axial symmetry of the charge distribution around the z-axis of the truncated cone. It is also found that the charge at the corner areas is concentrated and as the distance d gets smaller, the charge at the intersection of the side and bottom of the truncated cone is much greater than at the other corners. Based on the charge distribution, the capacitance between the truncated cone and the metal plate is found by Eq. (24) as shown in table 1.

The distance d is increased at 0.1mm intervals starting from d=1mm.

Table 1. Capacity value (unit pF) with distance d

d,mm	1.0	1.1	1.2	1.3	1.4	1.5	1.6	1.7	1.8	1.9	2.0
C, pF	4.833	4.692	4.566	4.452	4.349	4.254	4.167	4.087	4.013	3.944	3.843

From the calculated values of the table, it can be seen that the capacitance increases as the distance $d$decreases. To verify the accuracy of the calculated values, experiments are carried out in the next section and compared with the experimental values.

EXPERIMENTS AND DISCUSSION

The experimental setup is shown in Fig. 9. The dimensions of the truncated cone and metal plate are the same as in Section 2.

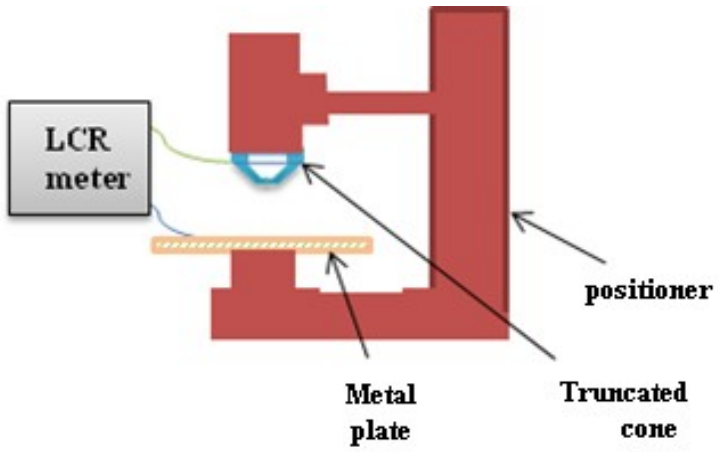

Fig.9. Experimental setup

In the experiment, the truncated cone was fixed to the movable rod with a fine-tuning screw, the metal plate was placed on the support, and the distance between the truncated cone and the metal plate was adjusted to 1mm. The capacitance value was measured, gradually increasing the distance. The distance d is increased at 0.1mm intervals starting from d=1mm. The capacitance values were measured with a LCR meter (U1731C, Malaysia, Agilent Technologies, resolution 0.01pF) and an electronic caliper (China, NingBo Industrial Tool Co., Ltd., resolution 0.01mm). The distance between the truncated cone and metal plate varies from 1mm to 2mm for V = 5.0V, R_1=8mm, R_2 =20mm, R_0 = 3mm and h = 10mm.

Table 2. Measured and calculated values with distance

d,mm / *C*,pF	1.0	1.1	1.2	1.3	1.4	1.5	1.6	1.7	1.8	1.9	2.0
C_{mea} (measured)	4.78	4.66	4.55	4.43	4.34	4.25	4.16	4.08	4.01	3.94	3.84
C_{cal} (computed)	4.833	4.692	4.566	4.452	4.349	4.254	4.167	4.087	4.013	3.944	3.879

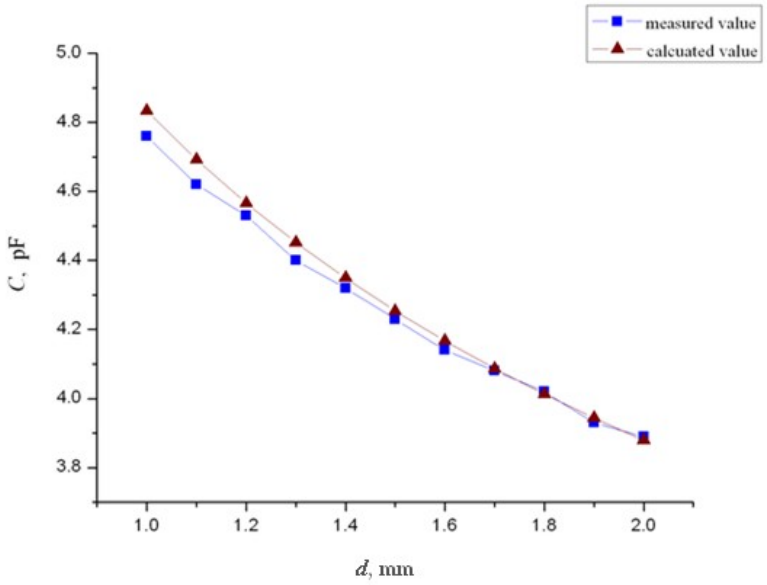

Fig.10. Experimental and calculated capacitance

The average relative error calculated from Table 2 is 0.24%. As can be seen from Tables 2 and Fig. 10, the measured and calculated values have a very good agreement. Thus, it is quite reasonable to estimate the capacitance of the system consisting of a truncated cone and a metal plate by the method of moments. The error between the calculated and measured values is attributed to the approximation method used when calculating the potential generated by the element at the observation point, instrument error, measurement environment, etc. if the element area is divided into finer or the distance between the truncated cone and the metal plate is much larger than the element surface, the result will be more accurate.

CONCLUSION

We have presented a method to evaluate the capacitance and charge distribution between the hollow metallic truncated cone and the metal plate using the method of moments in this paper. The accuracy of this method was verified by comparing the calculated and experimental values for a fixed value of h/R_1 ratio, R_2/R_1 ratio and R_1/R_0 ratio. In the future, we are going to further investigate the change characteristics of the capacitance and the error for differenth/R_1 ratio, R_2/R_1 ratio and R_1/R_0.

REFERENCES

Pal, A., & Vasuki, B. A concave electrode based capacitive sensor for cavitation monitoring-experimental evaluation. IEEE sensors journal, v. 20, p. 2094-2105, 2020.

Ubezio, B., Ergun, S., & Zangl, H. Realistic sensor simulations for the digital twin. Electrotech. Inftech., v. 140, p. 562-571, 2023.

Hanni, J.R., & Venkata, S.K. A novel helical electrode type capacitance level sensor for liquid level measurement. Sensors and Actuators, v. 315, p. 1-14, 2020.

Abdelhamid, H., Salem, T.Z., Wahba, M.A., Moded, D., Morsy, O.E., Abdelbaset, R., A capacitive sensor for differentiation between virus-infected and uninfected cells. Sensing and bio-sensing research, v. 36, p. 1-8, 2022.

Fu, Y.C., Fan, W., Jin, H.X., Chen, Q. A new capacitance angle sensor of concentric ring multi-layer differential. Measurement, v. 158, p. 1-8, 2020.

Harrington,R. F., Field Computation by Moment methods.IEEE Press,p. 35-82, 1993.

Savage,J. S.,&Smith, W. S. Capacitance calculation for cable harness using the method of moments.*IEEE Transactions on Electromagnetic Compat*ib*ility*, v.37, p. 131-137, 1995.

Das,B. N., Chkrabarty,S. B.,&Mallick,A. K.Moment method analysis of metallic cylinder and truncated cone used in orbital satellites.*Indian Journal of Radio and Space Physics*, v. 24, p. 151-157, 1995.

Mehta,P. D. &Chakrabarty,S. B., Electrical capacitance of dielectric coated metallic parallelepiped and closed cylinder isolated in free space.*Journal of Electrostatics*, v. 71, p. 756-762, 2013.

Hwang,C. O.&Michael,M., Electrical capacitance of unit cube.*Journal of Applied Physics*,v. 95, p. 3798-2802, 2004.

Das,B. N.,&Chakrabarty, S. B.Calculation of the Electrical Capacitance of a Truncated Cone.*IEEE Transactionson Electromagnetic Compatibility*, v. 39, p. 371-374,1997.

Chakrabarty,S. B., Das,S., &Das,B. N.Capacitance of Dielectric Coated Cylinder of Finite Axial Length and Truncated Cone Isolated in Free Space.*IEEE Transactions on Electromagnetic Compatibility*, v. 44, p. 394-398, 2002.

****